A DAMAGE TOLERANCE STUDY OF NOTCHED CFRP LAMINATES

M. Renault*, D. Valentin**, F. Perez***

The influence of progressive damage on the final failure of notched CFRP T300-914 is studied. Experimental results obtained at low loading, which correspond to an elastic behaviour present good agreement with the analytical and numerical results. The evolution of strain fields during the loading may be connected to the evolution of the damage state. The final failure load values, higher than expected, may be explained by the accumulation of damage prior to final failure. The behaviour differences between the lay-ups connected to the loading values at which damages appear and to the differences concerning their evolution. Then, it is shown that the capability of the point stress or average stress criterion to predict the final failure of notched sample depends on the damage development.

INTRODUCTION

Because of their high specific properties, carbon fibre reinforced plastic (CFRP) are more and more frequently used for applications in which weight gain becomes particularly significant. Their high anisotropy and the damage mechanisms involved do not allow to use with success the usual methods of notched structures design. The foreseen applications make necessary the development of more accurate methods. The aim of this study is to bring a better understanding of the influence of progressive damage on the final failure. In the following, the behaviour of notched CFRP T300-914 with different hole shapes are considered. Experimental results are compared to those obtained using theoritical and numerical methods.

* ENSMP-Centre des Matériaux P.M. Fourt - B.P. 87 91003 EVRY Cédex
** CNRS UA 866-Centre des Matériaux P.M. Fourt-B.P.87-91003 EVRY Cédex
*** AEROSPATIALE Les Mureaux - FRANCE.

GENERAL

Three kinds of notched laminates are studied : $(0,90)_s$, $(0,90,\pm 45)_s$ and $(0_3, 90, \pm 45)_s$. Sample's geometry is presented in figure 1. The aim of this study is to understand the influence of both sample width and thickness. Tests consist of static loading and the main techniques used for monitoring and observing damage are photoelasticimetry, strain gauges measurements, X radiography, as well as optical and scanning electron microscopy.

In the case of an elastic behaviour, the results may be compared to the analytical formulations obtained by the use of Lekhnitskü (1) and Sayers (2) results. For a notched sample, supposed to be thin, orthotropic and uniaxially loaded in its plan, the stress profile in the weakest section of the sample may be defined as follows :

- case of a hole with a radius R :

$$\sigma_y(x,\,o) = \sigma_{y\,o}\left\{1 + \frac{\beta_1^2}{(\beta_1-\beta_2)\,(1-\beta_1)}\left[1 - \frac{\beta_1 x}{\sqrt{R^2+\beta_1^2(x^2-R^2)}}\right] + \frac{\beta_2^2}{(\beta_1-\beta_2)\,(1-\beta_2)}\left[1 - \frac{\beta_2\, x}{\sqrt{R^2+\beta_2^2\,(x^2-R^2)}}\right]\right\}$$

this leads to a stress concentration factor :

$$K_T = 1 + \frac{\beta_1^2 + \beta_2^2}{\beta_1 - \beta_2} \qquad (2)$$

where β_1 and β_2 are solutions of :

$$\frac{1}{E_x}\beta^4 + \left(\frac{1}{G_{xy}} - \frac{2\nu_{xy}}{G_{xy}}\right)\beta^2 + \frac{1}{E_y} = 0 \qquad (3)$$

Expression (1) is available if $\beta_1 \neq \beta_2$. If $\beta_1 = \beta_2$, the isotropic case or the "quasi isotropic" case is found which leads to the expression (4).

$$\sigma_y(x,o) = \sigma_{y\,o}\left\{1 + \frac{1}{2}\left(\frac{R}{x}\right)^2 + \frac{3}{2}\left(\frac{R}{x}\right)^4\right\} \qquad (4)$$

which leads to a stress concentration factor equal to 3.

- case of a notch with a length 2 b.

$$\sigma_y(x,o) = \frac{K_I \; x}{\sqrt{\pi b \; (x^2 - b^2)}} \quad \text{with } K_I = \sigma_{y_o} \sqrt{\pi b} \quad \text{stress intensity factor.}$$

These results have been compared to those obtained using the finite element code ABAQUS. Shell elements with superimposed layers and reduced integration method were used. Each layer has a thickness and is considered as an orthotropic material defined with the values of the elastic constants in its orthotropy axis and the value of the angle between these axis and those of the general reference. An exemple of mesh which have been considered for this study is presented in figure 2.

ELASTIC BEHAVIOUR

During a static tension test, it can be seen that the sample behaviour remains elastic at the beginning of the test, next, when a sufficient loading is reached, a non linear behaviour is observed. The threshold values at which non linerity appears are determined by analysis of the strain fields, using photoelasticimetry, and by analysis of the non linearities on the (load-strain) curves obtained by extensometry.

For the $(0,90 \pm 45)_s$ lay-up, it can be noticed that the non linear behaviour appears only at about 70 or 80 % of the failure load value. On the contrary, for the two other lay-ups, this non linearity may appear as soon as the load values reach 20 or 30 % of the failure load. Otherwise, these results are not much dependant of the hole shape.

On figure 3, the good correlation between experimental, numerical and analytical results may be noticed as long as the behaviour is elastic. Moreover, the comparison between the stress concentration factor values obtained analytically or numerically bears out the fact that calculations describe correctly the elastic behaviour stage (table 1).

TABLE 1 - Analytical and numerical values of K_T

K_T	$(0,90)_s$	$(0,90 \pm 45)_s$	$(0_3, 90, \pm 45)_s$
analytical	4,95	3	4,4
numerical	5	2,95	4,5

When the sample behaviour stops being elastic, different non linearities on the curves (strain-load) may be observed. Main of them are presented in figure 4. In the areas localized near the weakest section of the sample, an apparent gain or loss of rigidity is observed, depending on wether the area is near or far from the hole. In the areas localized above or below the hole, a localunloading is observed. Practically, all the behaviour modifications are the consequences of local loss of material properties and of stress redistributions due to damage evolutions.

Macroscopic damage which can be observed before the final failure are matrix failures, parallel to fibres in the different ply orientations and delaminations near the hole and in areas where high fissuration densities exist in two adjacent plies. A schematical representation of these damage evolutions is presented in figure 5 in the case of $(0,90)_s$ and $(0,90, \pm 45)_s$ lay-ups with circular holes. It can be noticed that the use of a classical ply failure criterion (Tsai-Hill or Tsai-Wu criterion for exemple) and an analysis of the elastic results enable the prediction of the load level at which the first damage by matrix failure appears.

Concerning the $(0,90)_s$ lay-up, matrix failure parallel to fibres direction appears and propagates at low loads in the 90° plies, and tangentially to the hole in the 0° too. Then significant delaminations are detected near the hole and in the vicinity of the fissurations in the 0° plies. Concerning the $(0_3, 90, \pm 45)_s$ lay-up, damages are created ealy and propagate in a significant mamer. The main differences with $(0,90)_s$ lay-up are multiple matrix failures in the ± 45° plies, essentially above and below the hole and a greater delamination which may extend over all the areas between fissurations in the 0° plies. On the contrary, for the $(0,90, \pm 45)_s$ lay-up, damages appear later and their development are less significant. Moreover, it may be noticed that, for a given lay-up, delaminations are more significant when the ply thickness is greater. This may be explained by the higher energy in the sample which must be dissipated in the same number of interfaces. Local consequences of ply failures are essentially a loss of rigidity of the damaged ply in the direction perpendicular to the fibres and a reduction of stress transfer by shear within the ply. Otherwise, delaminations lead to a reduction of the lay-up moduli, and put a stop to the stress transfer by shear between the plies. Moreover, it must be remarked that all these developments are not independant and that the influence of each of them depends on the presence or not of other kinds of damages. Then, it is of interest to notice that the damaged material behaviour is an elastic damages behaviour as shown in figure 4, excepted in the areas above and below the hole. If the sample is unloaded and reloaded, the behaviour seems to be elastic as far as the maximum load value previously reached is not reaches. When load is removed, no residual strains are measured. Global influence of these damages may be very

important. The evolution of strain profiles in the weakest section of the sample during the loading are presented in figure 6 for the $(0,90)_s$ $(0,90, \pm 45)_s$ lay-ups. A behaviour difference may be observed, the change in strain profile appears later and is less significant for the $(0,90, \pm 45)_s$ lay-up. The analysis of all the obtained results enlighted the particular role of matrix failures which propagate in the 0° plies, where high stress transfers occur by shear between the areas above or below the hole and those on both sides of the hole. Their presence disturbs considerably these transfers, especially if there are delaminations too, and modify strain fields in the sample. Then the differences connected with strain profiles evolution and those connected with damage development for the different lay-ups may be correlated.

FAILURE STRESS VALUES

Actually, there are many methods for failure prediction of notched composite material. Most of them have been systematically tested in (3). Experimental results have been analyzed using the Whitney and Nuismer methods (4, 5). These methods assume that failure occurs either when the stress σ_y , over some distance, d_o, ahead of the discontinuity is equal to or greater than the strength of the unotched laminate, σ_o, (point stress criterion) or when the average stress, σ_y, over some distance, a_o, equals the value of σ_o (average stress criterion). The two parameters which must be determined are σ_o and d_o or a_o. They depend of the material, of the stacking sequence and of the hole shape. Results obtained with the $(0,90)_s$ and the $(0,90, \pm 45)_s$ lay-ups are presented in figure 7, these obtained with the $(0_3, 90, \pm 45)_s$ lay-up are very similar to those obtained with the $(0,90)_s$ lay-up. For the $(0,90, \pm 45)_s$ lay-up, a reduction of the failure stress value may be noticed when the hole size growths. This evolution is correctly described by the failure prediction methods. On the contrary, for the other lay-ups, there is no evolution of the failure stress value with the hole size and results obtained with the Whitney-Nuismer methods do not describe this phenomenon.Moreover, the failure stress value of the notched sample, taken into account its real section, is almost equal to those of the unotched sample. This different failure behaviour may be explained by the different damage states. So, presence of significant damage, which appears during the tests, contributes be modify the stress distributions and diminishes the stress concentrations near the hole. When the overstresses becomes very low, the sample behaviour is almost similar to that of two parallel unnotched samples tested in tension and the failure stress values may be almost equal to those of the unnotched samples. Therefore, the hole size influence becomes very low. On the contrary, if there is very few damage, there are signifcant stress concentrations over a distance which depends on the hole size. Then failures stress value in presence of a hole becomes than those of the unnoteched material and is a fonction of the hole size.

CONCLUSIONS

In the elastic case, analytical and numerical approach are in agreement with experimental results obtained on notched CFRP specimen tested in tension. However, non linearities are observed above thresholds which depend of the stacking sequences. They are due to plies failures and delaminations. The main effects are to reduce the overstresses in the vicinity of the hole. Their introductions in the failure prediction models should lead to a better accuracy.

AKNOWLEDGEMENT

This work has been supported by the Centre National d'Etudes Spatiales.

SYMBOLS USED

E_x, E_y : Young's modulus in the x and y direction (Pa)
G_{xy} : Shear modulus (Pa)
D_{xy} : Poisson coefficient
σ_y, σ_{yo} : Stress and failure stress in the y direction (Pa)
R : hole's radius (m)
b : half length of the notch (m)
K_T : stress concentration factor
K_I : stress intensity factor (Pa $\sqrt{m}$).

REFERENCES

(1) Lekhnitskii, S.G., "Theory of elasticity of an anisotropic body". Holdenday, San Francisco, 1963.

(2) Sayers, K.H., Beaulieu, C., Engrand, D., "Trou, calcul pratiques des composites". Composites n° 2, mars-avril 1984.

(3) D.F.V.L.R., "Development of fracture mechanics maps for composite materials". ESTEC contract n° 4825/81/NL/AK (SC), final report, Vol. 4.

(4) Whitney, J.M., Nuismer, R.J., "Stress fracture criteria for laminated composites containing stress concentrations". J. Composite Materials, Vol. 8, 1974.

(5) Whitney, J.M., Nuismer, R.J., "Uniaxial failure of composite laminates containing stress concentrations". Fracture mechanics of composite, ASTM STP 593, American Society of Testing and Materials, 1975, pp. 117-142.

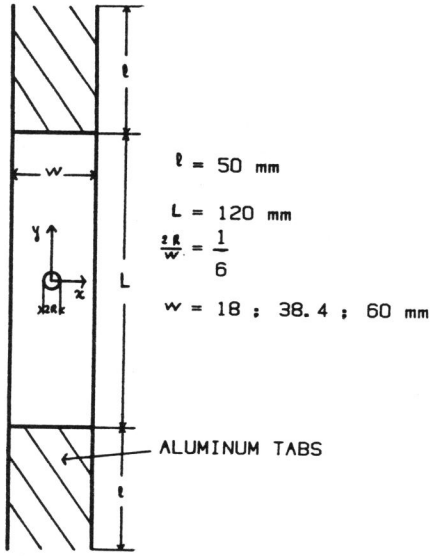

Figure 1 Sample's geometry.

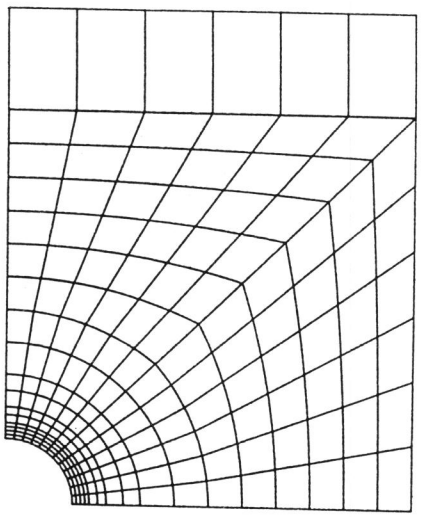

Figure 2 Exemple of mesh used during the study.

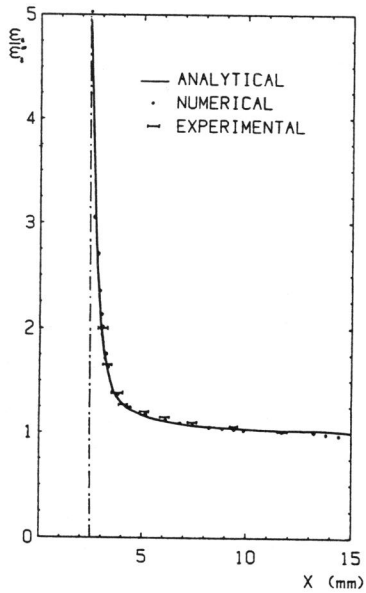

Figure 3 Strains profiles in the weakest section for the $(0,90)_s$ lay-up with circular hole.

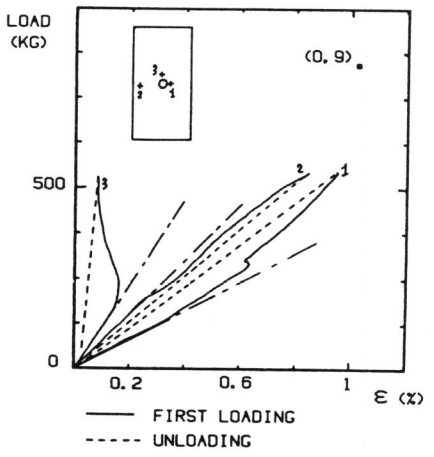

Figure 4 Main non-linearities which may be observed.

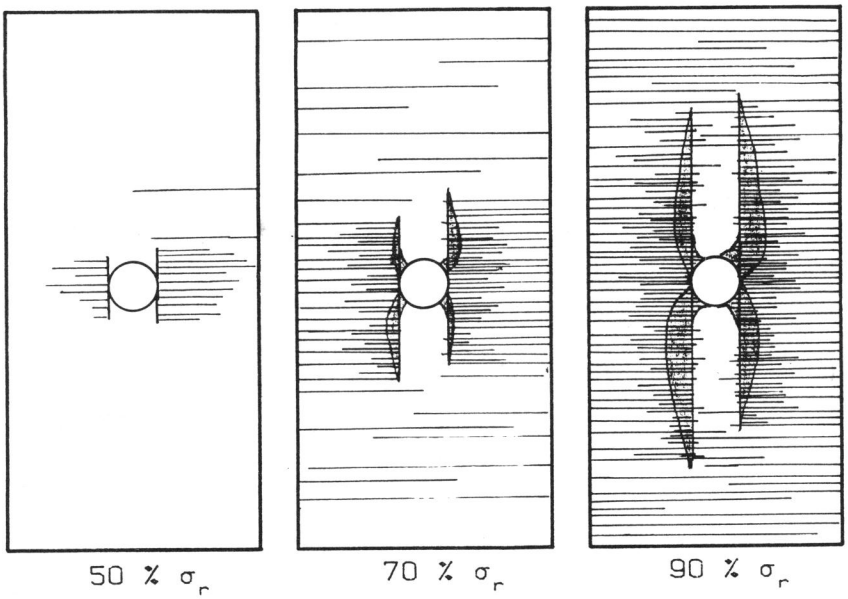

Figure 5a Damage evolution for the $(0,90)_s$ lay-up.

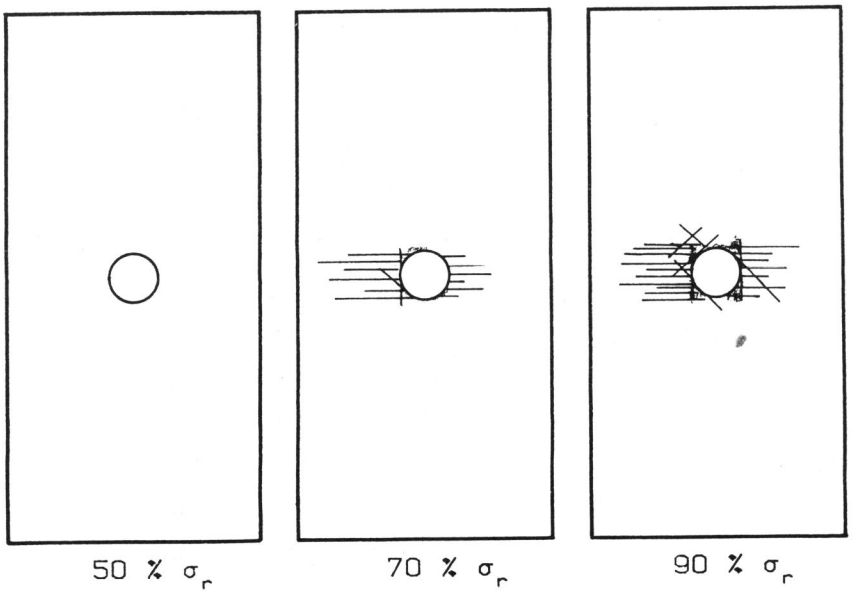

Figure 5b Damage evolution for the $(0,90, \pm 45)_s$ lay-up.

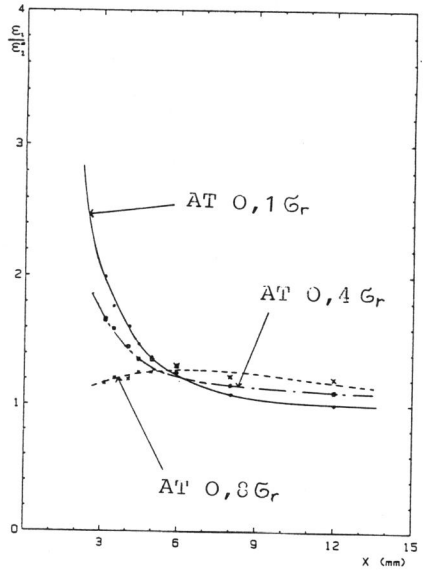

Figure 6a : Strains profile evolution for the $(0,90)_s$ lay-up.

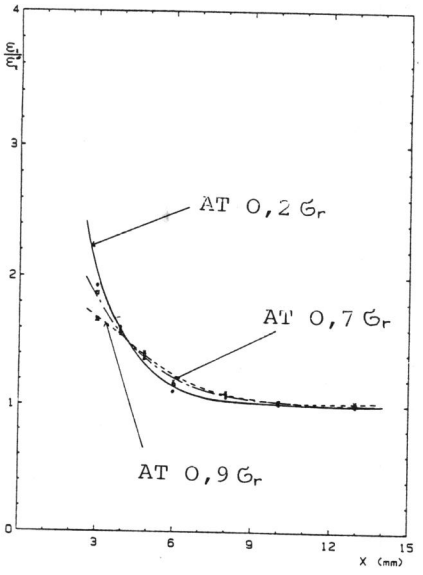

Figure 6b : Strains profile evolution for the $(0,90,\pm 45)_s$ lay-up.

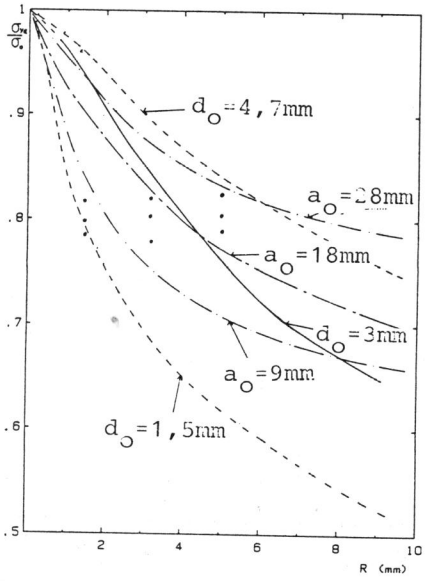

Figure 7a : Failure stress values for a $(0,90)_s$ lay-up with circular holes.

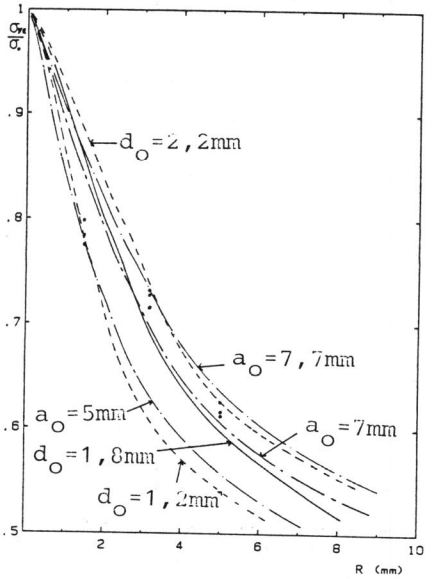

Figure 7b : Failure stress values for a $(0,90, \pm 45)_s$ lay-up with circular holes.